MATERIALS CHEMISTRY FRONTIERS

CCS 中国化学会 CHINESE CHEMICAL SOCIETY

ICCAS

ROYAL SOCIETY OF CHEMISTRY

Visible Light, Temperature, and Electric Field-Driven Rotation of Diffraction Gratings Enabled by an Axially Chiral Molecular Switch

Journal:	*Materials Chemistry Frontiers*
Manuscript ID	QM-RES-10-2022-001003.R1
Article Type:	Research Article
Date Submitted by the Author:	23-Oct-2022
Complete List of Authors:	Zhang, Xinfang; Kent State University Hassan, Fathy; Tanta University Faculty of Science, ; Kent State University, Bisoyi, Hari Krishna; Kent State University, Liquid Crystal Institute Wang, Hao; Kent State University, Liquid Crystal Institute and Chemical Physics Interdisciplinary Program Zhou, Ziyuan; Kent State University Li, Quan; Kent State University, Liquid Crystal Institute

ARTICLE

Visible Light, Temperature, and Electric Field-Driven Rotation of Diffraction Gratings Enabled by an Axially Chiral Molecular Switch

Received 00th January 20xx,
Accepted 00th January 20xx

DOI: 10.1039/x0xx00000x

Xinfang Zhang,‡[a] Fathy Hassan,‡[ab] Hari Krishna Bisoyi,[a] Hao Wang,[a] Ziyuan Zhou,[a] and Quan Li*[ac]

The design and development of functional soft materials with responsive and adaptive properties that can be driven by multiple stimuli are necessary for fundamental scientific enquiry and technological applications in advanced devices. Herein, a novel visible light responsive axially chiral molecular switch with high helical twisting power (HTP) has been synthesized which shows good compatibility in a commercially available nematic liquid crystal (LC) host E7. The cholesteric liquid crystal (CLC) mixture fabricated using the chiral switch and LC E7 can be driven by visible light, temperature, and electric field. Reversible red, green, and blue (RGB) reflection colors upon visible light irradiation and temperature variation are achieved in the planar cell. When the CLC mixtures with different concentrations of chiral switch are introduced into hybrid cells with planar and homeotropic boundary conditions spontaneous formation of diffraction gratings (DGs) occur. Good quality DGs are obtained in the range of ~1.85 ≤ d (cell thickness)/*P* ≤ ~4.30. The stripes rotate clockwise continuously with the maximum rotation angle over 2π (383.1°) upon visible light (405 nm) irradiation, over π (192.4°) upon increasing temperature, and over π/2 (101.2°) upon applying electric field, respectively. Such multi-stimuli (visible light, temperature, and electric field) responsive in-plane rotation of the DGs shows great potential for beam steering, spectrum scanning, and beyond.

1. Introduction

The design and synthesis of novel stimuli-responsive materials have been tremendously advocated in the application of optics and photonics devices.[1-9] Among optical devices, diffraction gratings (DGs) as a basic and important component, have been widely studied in the field of beam steering, spectrum scanning, etc.[10-14] Cholesteric liquid crystals (CLCs) with intrinsic self-organized helical superstructures, as one of prominent stimuli-driven functional materials, have been utilized for creating DGs.[15-29] The performance of cholesteric DGs is determined by several factors such as the surface alignment of substrates, the helical pitch (*P*) of CLCs, and so forth.[30-37] Compared with homogeneous alignment or vertical alignment on both substrates of cells, hybrid aligned boundary conditions with one planar aligned surface and another vertical aligned surface provide a spontaneously periodic distortion, resulting in striped domains of CLC gratings oriented unidirectionally.[38] The orientation of these stripes can be continuously rotated in hybrid aligned boundary conditions under different external stimuli, including light, temperature, and electric field. Lin et al.[39] reported the continuously rotatable CLC gratings with the rotation angle of about 101° under the thermal effect in a hybrid aligned cell with the mixture of liquid crystal (LC) E7 and chiral dopant CB15. The rotation angle about 48° of gratings was also achieved under an electric field in that system. Nose et al.[40] also observed the continuous rotation of striped domains of CLC gratings in hybrid aligned surface under applying electric fields, and the possible mechanism of stripe rotation was further investigated, including four stages: defect creation, moving and connection shift, recombination, and relaxation and rotation. Light irradiation is also used effectively to manipulate the rotation of CLC gratings based on photoresponsive chiral molecules.[41] The helical twisting power (HTP), increases or decreases under light irradiation via changing the pitch length owing to photoisomerization of the photoresponsive chiral dopants which twist the nematic host. A planar chiral cyclic azobenzene was synthesized and doped into LC 5CB to obtain a cholesteric film.[42] A full cycle (360°) of rotational motion of a micron-size glass rod was achieved under UV light irradiation. A CLC system with two dopants of opposite chirality exhibited a broad change in helical pitch and a reversible inversion of helix handedness.[43] Accordingly, the continuous rotation angle of CLC gratings was about 690°, while the total rotation was up to about 1220° under the UV light irradiation. Further, visible light-driven rotation of CLC gratings with a commercially available azobenzene chiral dopant ChAD-3c-S (BEAM) was also investigated in semi-free films, in which the substrate is planar aligned and the air/LC interface is near-vertical.[44] The maximum continuous rotation angle was up to 987.8° through a bandpass filter (450-490 nm). However, such open CLC films can be easily

[a] *Advanced Materials and Liquid Crystal Institute and Materials Science Graduate Program, Kent State University, Kent, Ohio 44242, USA*
[b] *Department of Chemistry, Faculty of Science, Tanta University, Tanta, El-Gharbia 31527, Egypt*
[c] *Institute of Advanced Materials and School of Chemistry and Chemical Engineering, Southeast University, Nanjing, Jiangsu 211189, China. *E-mail: quanli3273@gmail.com*

† Electronic supplementary information (ESI) available. See DOI: 10.1039/x0xx00000x

‡ X. Zhang and F. Hassan contributed equally to this work.

contaminated and wetted because the upper surface was in contact with air. While cholesteric gratings that can be driven by a single stimulus have become common, the development of tunable cholesteric gratings that can be effectively driven by multiple stimuli either independently or in combination is imperative to explore their full potential under diverse operating conditions.

Here, we report the synthesis and characterization of a novel molecular switch (*R*)-**1** as a photoresponsive chiral dopant with an extended π-conjugated structures. This molecular design results in good compatibility and high HTP in achiral nematic host and exhibits visible-visible light-driven behavior for photoisomerization process instead of UV light which was necessary to drive the classical molecular switches at least in one direction. The utility of using visible-light is not only to avoid the harmful irradiation of UV light which degrades both materials and operating system but also promising for impeding these materials in advanced photonic devices for future applications.[45-48] Reversible red, green, and blue (RGB) reflection colors upon visible light irradiation and temperature variation in a planar cell with CLC mixture of (*R*)-**1** and LC E7 are demonstrated. Visible light, temperature, and electric field-driven rotation of diffraction gratings in hybrid aligned cells with different initial pitch lengths of CLC mixture are obtained, exhibiting that the stripes rotate clockwise continuously with the maximum rotation angle over 2π (383.1°) upon visible light (405 nm) irradiation, over π (192.4°) upon increasing temperature, and over π/2 (101.2°) upon applying electric fields, respectively. Furthermore, we demonstrate multi-stimuli (visible light, temperature, and electric field) responsive rotatable diffraction patterns with two probing beams (red laser and unpolarized collimated white-light), which has potential applications in non-mechanical in-plane beam steering and spectrum scanning.

2. Results and discussion

2.1. Photoisomerization behavior and chiral induction ability of chiral switch (*R*)-1

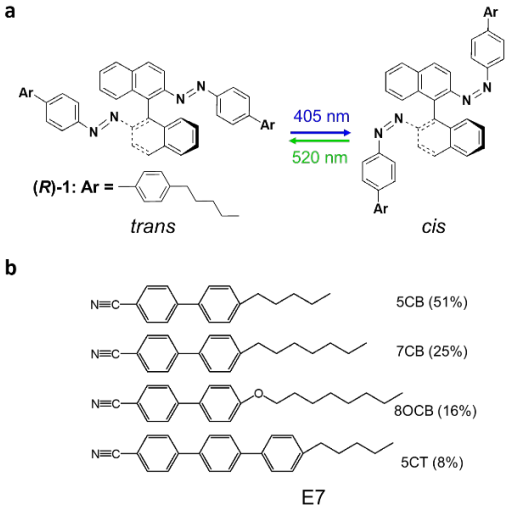

Fig. 1 Chemical structure of (a) the chiral molecular switch (*R*)-**1** undergoing reversible *trans-cis* photoisomerization by visible light irradiation (405 nm and 520 nm) and (b) the nematic liquid crystal mixture E7 used in this study.

The chiral molecular switch (*R*)-**1** was synthesized facilely (Scheme S1†). The chemical structure undergoing reversible *trans-cis* photoisomerization by visible light irradiation (405 nm and 520 nm) is shown in Fig. 1a. The directly attached pentylbiphenyl groups at para position leads to an extended π-conjugation structure and a maximum absorption band around 365 nm.

Reversible *trans-cis* photoisomerization upon visible light (405 nm and 520 nm) irradiation in 1,4-dioxane was observed via UV-Vis absorption and circular dichroism (CD) spectra (Fig. 2a and 2c, respectively). The intensity of the maximum absorption band at around 365 nm (π-π* transition) decreased while the intensity of the weak absorption band at around 470 nm (n-π* transition) increased upon visible light irradiation at 405 nm owing to the *trans*-to-*cis* photoisomerization. The CD spectra exhibited exciton couplets at 220 nm and 360 nm, which were derived from the ^1B_b and ^1L_b transitions of the 1,1'-binaphthyl.[49] We also detected exciton couplets of the azo unit at 415 and 475 nm, which corresponded to the π-π* and n-π* transitions, respectively. A photostationary state (PSS) by 405 nm irradiation was obtained after 3 min exposure. The reverse *cis*-to-*trans* photoisomerization is obtained under green light irradiation at 520 nm for 3 min. Moreover, we also explored the variation at 365 and 470 nm of absorption intensities and 360 and 415 nm of CD spectra in ten cycles via alternating visible light irradiation with two different wavelengths (405 nm and 520 nm) as shown in Fig. 2b and Fig. 2d, respectively. These results confirm that the photo-switchable (*R*)-**1** exhibits the ability to achieve reversible photoisomerization upon visible light irradiation and good fatigue resistance after ten cycles of irradiation. We also investigated *trans*:*cis* isomers ratios in PSS by ^{1}H-NMR spectroscopy. Under irradiation at 405 nm for 30 min, a decrease in the intensity of ^{1}H-

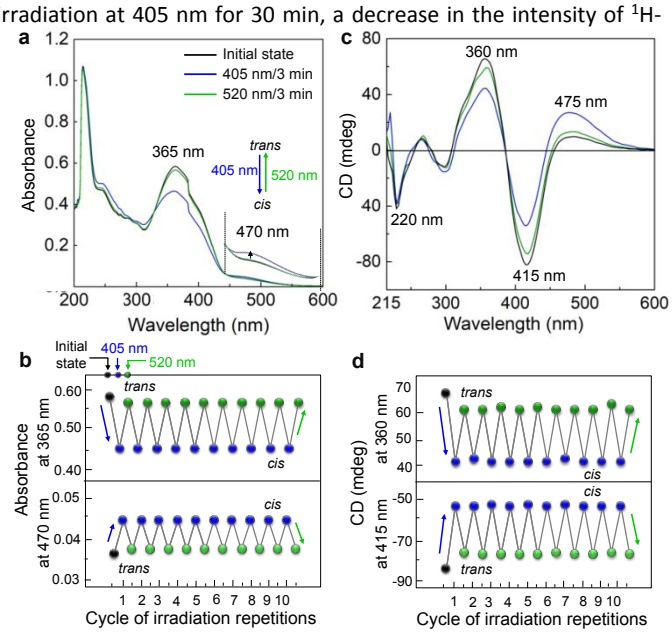

Fig. 2 (a) UV-Vis absorption spectra of the chiral molecular switch (*R*)-**1** in 1,4-dioxane (0.5×10^{-5} M). The region in the range of 440-590 nm of the spectra is magnified. (b) Photoswitchable behavior of absorbance (monitoring wavelengths: 365 and 470 nm). (c) CD spectra in 1,4-dioxane (0.5×10^{-3} M). (d) Chiroptical switching behavior (monitoring wavelengths: 360 and 415 nm). Visible light (405 nm, 1.5 mW cm^{-2} and 520 nm, 2.2 mW cm^{-2}), repeated cycle of irradiation (3 min, 10 cycles).

NMR peaks of the hydrogen atoms close to the azo group and

appearances of new peaks of *cis* H_a and *cis* H_b were observed (Fig. S1†). The ratio of *trans*:*cis* isomers in PSS were calculated to be 74:26. ^{1}H-NMR peaks were almost recovered to the initial state under visible light irradiation by 520 nm in PSS (*trans*:*cis* = 97:3).

Further, the directly attached pentylbiphenyl groups at para position resulted in good compatibility in LC hosts. The homogeneous CLC mixture was prepared by doping chiral molecular switch (*R*)-**1** into the commercially available nematic LC host E7 (Fig. 1b). The ability of the chiral molecular switch (*R*)-**1** to twist nematic LC host E7 was studied. The initial helical pitch (*P*) of the CLC mixture (0.36 wt% (*R*)-**1** in E7) and the pitch variations resulting from *trans-cis* photoisomerization upon visible light (405 nm, 1.5 mW cm^{-2} and 520 nm, 2.2 mW cm^{-2}) irradiation and temperature variation were investigated by the traditional Grandjean-Cano method in a wedge cell (EHC, KCRK-07, tanθ = 0.0196) (Fig. 3a and Fig. 3b). The helical twisting power (HTP, μm^{-1}) (Table 1) was calculated according to HTP=1/(c·*P*), where "c" is the concentration of the chiral molecular switch. In the initial state (25 °C), the HTP is 104 μm^{-1}. Due to the *trans*-to-*cis* photoisomerization, the HTP decreased to 71 μm^{-1} upon 405 nm visible light irradiation. Following 520 nm visible light exposure, the HTP increased to 92 μm^{-1}. Moreover, when the temperature was increased from 25 °C to 56 °C, the HTP decreased to 80 μm^{-1}, and there is a phase transition observed from cholesteric phase to isotropic phase at around 56.2 °C. The reason of HTP varying with temperature is that as the temperature increases, the conformation of the chiral molecule changes resulting in the variation of intermolecular interaction between the chiral dopant and the host.[50]

Table 1. HTP (wt%, μm^{-1}) of (*R*)-**1** in E7 host before and under visible light irradiation (405 nm, 1.5 mW cm^{-2} and 520 nm, 2.2 mW cm^{-2}) and under temperature variation as determined by Grandjean-Cano method in a wedge cell.

	HTP (wt%, μm^{-1})		
Visible light	**Initial state**	**PSS$_{405\ nm}$**	**PSS$_{520\ nm}$**
	104	71	92
Temperature	**25 °C**	**56 °C**	**~56.2 °C**
	104	80	Phase transition

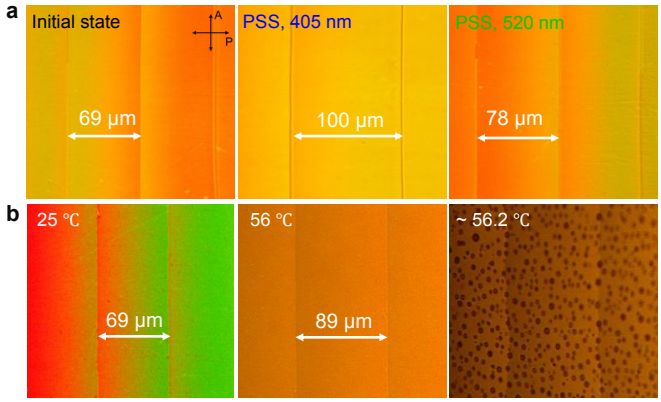

Fig. 3 (a) POM images of CLC mixture (0.36 wt% (*R*)-**1** in E7 host in a wedge cell before and under visible light irradiation (initial state, PSS$_{405nm}$ and PSS$_{520nm}$) and (b) under temperature variation (25 °C, 56 °C, and ~56.2 °C).

The handedness of CLC mixture was determined by the miscibility test performed between sample mixture (0.96 wt% (*R*)-**1** in E7) and the standard compound cholesteryl oleyl carbonate (left-handed).[47] If the chirality of the test sample is same as the standard sample, the mixing boundary will be continuous. Conversely, different chirality of the test sample will lead to a nematic gap. As shown in Fig. S2†, a gap existed in the mixing region which meaning that CLC mixture containing chiral molecular switch (*R*)-**1** possesses right-handedness. Further, a high concentration of CLC mixture containing 3.4 wt% (*R*)-**1** in E7 was prepared. At this concentration, the corresponding pitch is around 282 nm according to the HTP value, and the resulting mixture is homogeneous without phase separation due to the good compatibility of (*R*)-**1** in E7 owing to the molecular design. After this mixture was filled into a planar cell with the back substrate painted black, we observed a blue selective reflection color. A 3D goggle with left glass transmitting the left-circular polarized light and right glass transmitting the right-circular polarized light was used to observe this planar cell. The circularly polarized light can be reflected from CLC with the same handedness of the helical superstructure, and the reflective blue color can be only seen from the right glass (Fig. S3†). Thus, this proved that the chiral molecular switch (*R*)-**1** induces a right-handedness in E7.

2.2. Photochemically and thermally driven RGB colors of CLC

The potential application of tunable RGB (red, green, and blue) reflection colors was explored in a planar cell (INSTEC, 5.0 μm cell gap). Based on the variation of HTP upon visible light irradiation and temperature, photochemically and thermally driven RGB colors in a planar cell filled with 3.4 wt% molecular switch (*R*)-**1** in E7 were achieved, and the real reflective color of the cell and the corresponding reflection spectra were recorded. The central reflection wavelength and the pitch of CLC are related by the equation λ = n·*P*, where "n" is the average refractive index of the LC. As shown in Fig. S4a†, the initial central reflection wavelength is around 450 nm, and the cell reflects the blue light (405 nm, 0 s). Upon 405 nm irradiation (1.5 mW cm^{-2}), the central reflection wavelength shifted from 450 nm (blue) to 530 nm (green), and finally to 650 nm (red) at photostationary state (PSS, 120 s). Following 520 nm irradiation (2.2 mW cm^{-2}), the reverse process across RGB reflection colors was observed. Moreover, the reversible reflection color of CLC across RGB bands was also tuned by temperature (Fig. S4b†). However, the tuning of reflection colors of this standard CLC cannot be observed via increasing electric fields gradually (Fig. S5†), due to a transition from planar state to focal conic state with the random distribution of helical axis, finally to homeotropic state. From these results, we conclude that the CLC mixture containing chiral molecular switch (*R*)-**1** shows great of interest for photochemically and thermally driving RGB colors with efficient reversibility.

2.3. Multi-stimuli (visible light, temperature, and electric field) responsive rotatable in-plane CLC gratings

The CLC mixtures with different concentrations of chiral dopant were introduced into hybrid-aligned cells to obtain the CLC gratings. One substrate of the hybrid cell shows vertical

alignment, providing a parallel helical axis of CLC with the substrate, while another substrate shows planar alignment, providing a perpendicular helical axis with the substrate (Fig. 4a). It should be noted that the good quality of CLC gratings can be optimized via adjusting the ratio of d/*P*.[39] In this study, CLC mixtures with different concentrations of chiral dopant were filled into hybrid cells with same cell thickness (d = 5 μm). The good quality of initial stripe domains of CLC gratings can be observed in the range of ~1.85 ≤ d/*P* ≤ ~4.30 without any external stimuli (Fig. S6†). Further, the stripe direction of CLC grating can be rotated in the plane via different external stimuli, and the total in-plane rotation angle depends on several parameters, like the elastic property of LC host, the ratio of d/*P*, the interaction between LC and chiral molecules, and the surface anchoring energy of the substrate. From the measurements in the wedge cell, the pitch of CLC was manipulated with visible light and temperature continuously. Moreover, LC molecules are very sensitive to the weak alternating current (AC), by virtue of the inherent dielectric anisotropy (Δε), enabling reorientation of the helical axis of CLC mixture. Therefore, triple external stimuli including visible light, temperature, and electric field were applied respectively in this work to rotate the stripes of CLC gratings.

The total rotation angle of CLC gratings with different initial d/*P* values under each external stimulus (visible light, temperature, and electric field) are shown in Fig. 4b. It can be observed that the total rotation angle of CLC grating is directly proportional to the initial d/*P* value upon visible light irradiation (405 nm) and increasing temperature. The reason is that a larger initial d/*P* value possesses a smaller pitch and more CLC layers, and the total rotation angle of CLC grating is the variational sum of helical pitch of CLC layers, thus, a larger initial d/*P* value causes a larger rotational angle. However, the rotation angle decreases with initial d/*P* value upon applying electric field. The threshold voltage of phase transition from cholesteric phase to nematic phase is inversely proportional to the helical pitch.[51,52] A smaller initial d/*P* value possesses a larger pitch and a lower phase-transition voltage, thus, the helical structure can be easily unwound, resulting in the large rotational angle at a small d/*P* ratio.

Fig. 4c-e shows POM images of the continuous rotation process of the CLC grating with maximum rotation angles upon three external stimuli respectively. For the visible light irradiation (405 nm, 1.5 mW cm^{-2}) at the initial d/*P* ratio of 4.30, the stripes rotated clockwise continuously with the rotation angle of 383.1° due to the continuous increase of the helical pitch of CLC (Fig. 4c). The CLC grating can be fully rotated over

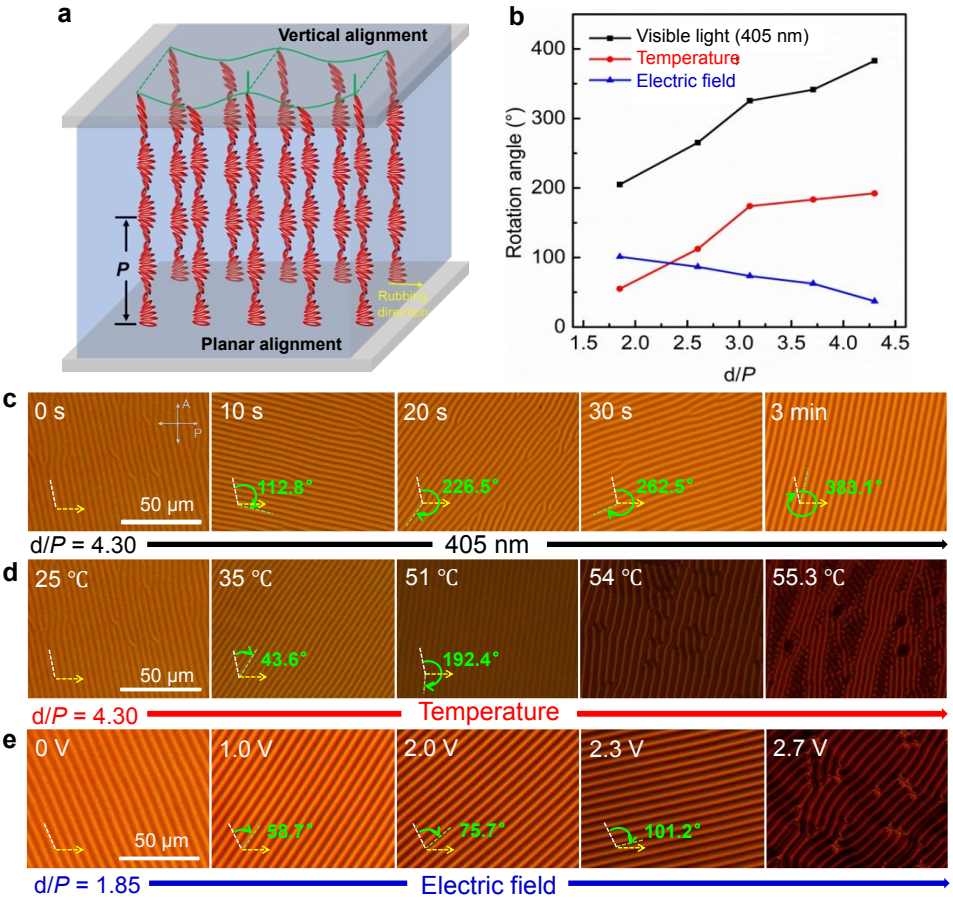

Fig. 4 (a) Schematic of the helical structure of CLC in a hybrid cell (*P*: helix pitch); (b) total rotation angle of the CLC gratings changing with different initial d/*P* values under triple external stimuli (visible light, temperature, and electric field). POM images of the continuous rotation process of the CLC grating (c) by visible light irradiation (405 nm,1.5 mW cm^{-2}) at the initial d/*P* ratio of 4.30, (d) with increasing temperature at the initial d/*P* ratio of 4.30, and (e) when applying electric fields at the initial d/*P* ratio of 1.85. (The yellow arrow represents the rubbing direction of the planar alignment layer, the white dotted line and the green dotted line represent the initial and the final stripe direction of CLC grating, respectively).

2π upon 405 nm visible light irradiation, and the reversible counterclockwise rotation process can be achieved by 520 nm light irradiation (Fig. S7†). The largest rotation angle of CLC grating driven by temperature was also obtained at the initial d/*P* ratio of 4.30, and the rotation process is shown in Fig. 4d, which was also continuous and clockwise because the pitch increased when the temperature increased. When the temperature reached to 51 ℃, the rotational angle was 192.4° (over π). Following a higher T, the CLC grating was not uniform due to the thermal fluctuation and when the T increased to about 55.3 ℃, the stripes started to fade away until completely black (isotropic phase). Electric field as the third driving force can also rotate the CLC grating with a largest rotation angle of 101.2° (over π/2) at the initial d/*P* ratio of 1.85. The pitch also increased with electric field, so the CLC grating was observed to continuously rotate clockwise as shown in Fig. 4e. Both initial states of CLC gratings can be restored after the removal of hot stage and electric field and putting the sample cell in the dark place for a couple of days. Although the maximum rotation angle (383.1°) upon 405 nm light irradiation obtained in this work is smaller than that (about 690°) under UV light irradiation[43] and that (987.8°) of a semi-free film through a bandpass filter (450-490 nm)[44], we achieved full 360° rotation of CLC grating in a hybrid cell by visible light irradiation. Further, compared with the values of rotation angles driven by temperature (101°) and electric field (48°) as reported[39], we achieved almost twice the rotation angles. From these results, we have achieved the multi-stimuli responsive rotations of CLC gratings with considerable rotation angles in the hybrid cell with the mixture of molecular switch (*R*)-**1** and LC E7. In addition, such CLC grating shows good fatigue resistance under the three different external stimuli respectively (Fig. S8†).

2.4. Applications in in-plane beam steering and chromatic dispersion for spectrum scanning

The potential application in non-mechanical in-plane beam steering of this multi-stimuli responsive rotation of CLC grating with the chiral molecular switch (*R*)-**1** in E7 was explored. The red laser diode (633 nm, 1 mW) as probing beam was applied (Fig. 5a). Furthermore, dispersion across the whole visible wavelength was observed when an unpolarized collimated white light with a pinhole was incident normally onto the hybrid cell (Fig. 5b). Upon the exposure of 405 nm light, the diffraction beam rotated clockwise continuously (Fig. 5c) along with the rotation of CLC grating (Fig. S9†). This colorful diffraction beam also rotated clockwise continuously along with the rotation of CLC grating upon 405 nm light irradiation (Fig. 5d). When the pinhole was replaced with a rectangular slit (Fig. S10†), the same rotation phenomenon was observed, while these wavelength components overlapped when the stripe direction of CLC grating is perpendicular to the long axis of the

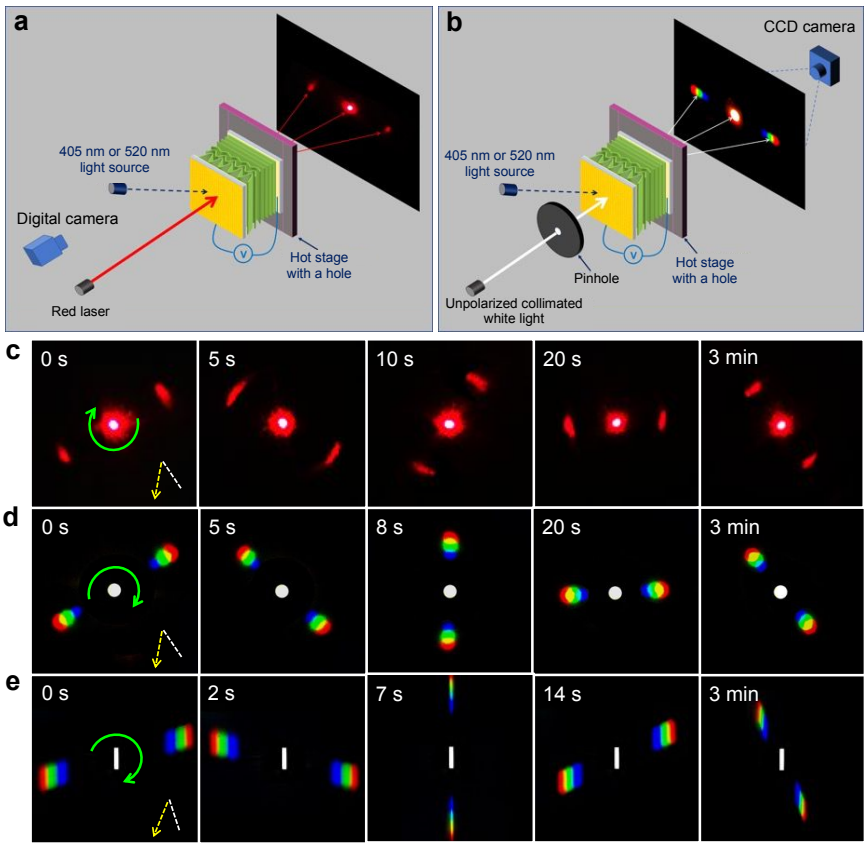

Fig. 5 Schematic illustration of diffraction experiment set-up with (a) the red laser diode (633 nm, 1 mW) and (b) the unpolarized collimated white-light as probing beams. Diffraction patterns with the initial d/*P* of 2.60 by (c) the red laser diode obtained via digital camera, and by the unpolarized collimated white light with (d) a pinhole and (e) a rectangular slit obtained via CCD camera, driven by visible light with the wavelength of 405 nm (1.5 mW cm^{-2}). (The yellow arrow represents the rubbing direction of the planar alignment layer, and the white dotted line represents the initial stripe direction of CLC grating).

rectangular slit (Fig. 5e). Similarly, the clockwise continuous rotation of diffraction patterns with two probing beams can be obtained under the driving of temperature and electric field (Fig. S11 and Fig. S12†). This kind of triple-induced manipulation of the CLC helical axis shows great potential in non-mechanical in-plane beam steering and chromatic dispersion for spectrum scanning.

3. Conclusions

We have designed, synthesized, and characterized a novel axially chiral molecular switch containing two azo linkages directly attached to the pentylbiphenyl groups. This chiral molecular switch shows reversible *trans-cis* photoisomerization upon visible light irradiation, good compatibility, and high HTP in achiral LC host E7. Photochemically and thermally driven reversible RGB reflection colors have been achieved in such CLC mixture with short pitch. The CLC mixture made by mixing different concentrations of chiral molecular switch (*R*)-**1** and E7 can spontaneously form unidirectional oriented stripe domains as diffraction gratings in the hybrid cell. The quality of such diffraction gratings is superior in the range of ~1.85 ≤ d/*P* ≤ ~4.30. The stripes rotate clockwise continuously with the maximum rotation angle over 2π (383.1°) upon visible light (405 nm) irradiation, over π (192.4°) upon increasing temperature, and over π/2 (101.2°) upon applying electric fields, respectively. Accordingly, we have achieved multi-stimuli (visible light, temperature, and electric field) responsive rotatable in-plane beam steering, and chromatic dispersion with white light source for spectrum scanning in these tunable cholesteric gratings. The materials developed here could find application in beam steering, spectrum scanning and other adaptive optical devices.

Author Contributions

Q. L. directed and designed the project. F. H. synthesized and characterized (*R*)-**1**， and studied the photoisomerization and chiral induction behaviors. X. Z. investigated the photochemically and thermally driven RGB colors, and the multi-stimuli (visible light, temperature, and electric field) responsive rotatable in-plane CLC gratings and prepared the first draft for the manuscript. X. Z. and Z. Z. achieved the applications in in-plane beam steering and chromatic dispersion for spectrum scanning. H. W. and H. K. B. contributed to the manuscript writing. H. K. B., H. W., and Z. Z. provided suggestions on the experiments. All authors discussed the progress of the research and reviewed the manuscript.

Conflicts of interest

The authors declare no competing interests.

Acknowledgements

The authors thank the support from the Air Force Research Laboratory and the Air Force Office of Scientific Research. The Fulbright Scholar Program, U.S. Department of State for the support to F.H. is acknowledged. We thank Dr. Dirk Friedrich and Dr. Farid Fouad for assistance for HRMS analysis.

4. References

1 Q. Li (ed.), Photoactive Functional Soft Materials: Preparation, Properties, and Applications, Wiley-VCH, Weinheim, 2019.
2 Q. Li (ed.), Intelligent Stimuli-Responsive Materials: From Well-Defined Nanostructures to Applications, ed. Q. Li, Wiley, Hoboken, 2013.
3 H. K. Bisoyi and Q. Li, Light-driven liquid crystalline materials: from photo-induced phase transitions and property modulations to applications, *Chem. Rev.*, 2016, **116**, 15089-15166.
4 H. K. Bisoyi and Q. Li, Light-directed dynamic chirality inversion in functional self-organized helical superstructures, *Angew. Chem. Int. Ed.*, 2016, **55**, 2994-3010.
5 Z. G. Zheng, R. S. Zola, H. K. Bisoyi, L. Wang, Y. Li, T. J. Bunning and Q. Li, Controllable dynamic zigzag pattern formation in a soft helical superstructure, *Adv. Mater.*, 2017, **29**, 1701903.
6 Z. G. Zheng, Y. Li, H. K. Bisoyi, L. Wang, T. J. Bunning and Q. Li, Three-dimensional control of the helical axis of a chiral nematic liquid crystal by light, *Nature*, 2016, **531**, 352-356.
7 K. Rijeesh, P. K. Hashim, S.-i. Noro, N. Tamaoki, Dynamic induction of enantiomeric excess from a prochiral azobenzene dimer under circularly polarized light, *Chem. Sci.*, 2015, **6**, 973-980.
8 R. S. Zola, H. K. Bisoyi, H. Wang, A. M. Urbas, T. J. Bunning and Q. Li, Dynamic control of light direction enabled by stimuli-responsive liquid crystal gratings, *Adv. Mater.*, 2019, **31**, 1806172.
9 M. Czajkowski, J. Klajn, J. Cybińska, J. Feder-Kubis and K. Komorowska, Cholesteric gratings induced by electric field in mixtures of liquid crystal and novel chiral ionic liquid, *Liq. Cryst.*, 2017, **44**, 911-923.
10 H. C. Jau, Y. Li, C. C. Li, C. W. Chen, C. T. Wang, H. K. Bisoyi, T. H. Lin, T. J. Bunning and Q. Li, Light-driven wide-range nonmechanical beam steering and spectrum scanning based on a self-organized liquid crystal grating enabled by a chiral molecular switch, *Adv. Opt. Mater.*, 2015, **3**, 166-170.
11 H. C. Jau, T. H. Lin, R. X. Fung, S. Y. Huang, J. H. Liu and A. Y. G. Fuh, Optically-tunable beam steering grating based on azobenzene doped cholesteric liquid crystal, *Opt. Expres*s, 2010, **18**, 17498-17503.
12 O. D. Lavrentovich, S. V. Shiyanovskii and D. Voloschenko, Fast beam steering cholesteric diffractive devices, *Proc. SPIE*, 1999, **3787**, 149-155.
13 H. C. Jau, T. H. Lin, Y. Y. Chen, C. W. Chen, J. H. Liu and A. Y. G. Fuh, Direction switching and beam steering of cholesteric liquid crystal gratings, *Appl. Phys. Lett.*, 2012, **100**, 131909.
14 A. Y. G. Fuh, C. H. Lin and C.Y. Huang, Dynamic pattern formation and beam-steering characteristics of cholesteric gratings, *Jpn. J. Appl. Phys*., 2002, **41**, 211.
15 R. Thomas, Y. Yoshida, T. Akasaka and N. Tamaoki, Influence of a change in helical twisting power of photoresponsive chiral dopants on rotational manipulation of micro-objects on the surface of chiral nematic liquid crystalline films, *Chem. Eur. J.*, 2012, **18**, 12337-12348.
16 D. Subacius, P. J. Bos and O.D. Lavrentovich, Switchable diffractive cholesteric gratings, *Appl. Phys. Lett*., 1997, **71**, 1350-1352.
17 J. J. Wu, Y. S. Wu, F. C. Chen and S. H. Chen, Formation of phase grating in planar aligned cholesteric liquid crystal film, *Jpn. J. Appl. Phys.*, 2002, **41**, L1318.
18 J. J. Wu, F. C. Chen, Y. S. Wu and S. H. Chen, Phase gratings in pretilted homeotropic cholesteric liquid crystal films, *Jpn. J. Appl. Phys.*, 2002, **41**, 6108.

19 I. A. Yao, C. H. Liaw, S. H. Chen and J. J. Wu, Direction-tunable cholesteric phase gratings, *J. Appl. Phys.*, 2004, **96**, 1760-1762.
20 A. Ryabchun, D. Yakovlev, A. Bobrovsky and N. Katsonis, Dynamic diffractive patterns in helix-inverting cholesteric liquid crystals, *ACS Appl. Mater. Interfaces*, 2019, **11**, 10895-10904.
21 Y. Shen, Y. C. Xu, Y. H. Ge, R. G. Jiang, X. Z. Wang, S. S. Li and L. J. Chen, Photoalignment of dye-doped cholesteric liquid crystals for electrically tunable patterns with fingerprint textures, *Opt. Express*, 2018, **26**, 1422-1432.
22 H. K. Bisoyi and Q. Li, Liquid crystals: versatile self-organized smart soft materials, *Chem. Rev.*, 2022, **122**, 4887-4926.
23 B. I. Senyuk, I. I. Smalyukh and O. D. Lavrentovich, Switchable two-dimensional gratings based on field-induced layer undulations in cholesteric liquid crystals, *Opt. lett.* 2005, **30**, 349-351.
24 I. Gvozdovskyy, O. Yaroshchuk, M. Serbina and R. Yamaguchi, Photoinduced helical inversion in cholesteric liquid crystal cells with homeotropic anchoring, *Opt. Express*, 2012, **20**, 3499-3508.
25 L. L. Ma, S. S. Li, W. S. Li, W. Ji, B. Luo, Z. G. Zheng, Z. P. Cai, V. Chigrinov, Y. Q. Lu, W. Hu and L. J. Chen, Rationally designed dynamic superstructures enabled by photoaligning cholesteric liquid crystals, *Adv. Opt. Mater.*, 2015, **3**, 1691-1696.
26 A. Kausar, H. Nagano, Y. Kuwahara, T. Ogata and S. Kurihara, Photocontrolled manipulation of a microscale object: a rotational or translational mechanism, *Chem. Eur. J.*, 2011, **17**, 508-515.
27 A. S. Zolot'ko, V. F. Kitaeva, N. N. Sobolev, V. Y. Fedorovich and N. M. Shtykov, Photoinduced periodic grating in cholesteric liquid crystals, *JETPL*, 1986, **43**, 614.
28 H. Espinet, M. Lesiecki and M. Ramsburg, Laser-induced gratings in nematic/cholesteric mixtures, *Appl. Phys. Lett.*, 1987, **50**, 1924-1926.
29 A. Y. G. Fuh, T. H. Lin, Y. Y. Chen, C. C. Li and H. C. Jau, Optical control of the rotation of cholesteric liquid crystal gratings, *Opt. Express*, 2019, **27**, 10806-10812.
30 I. Gvozdovskyy, Electro-and photoswitching of undulation structures in planar cholesteric layers aligned by a polyimide film possessing various values of the anchoring energy, *Liq. Cryst.*, 2018, **45**, 536-552.
31 I. Nys, K. Chen, J. Beeckman and K. Neyts, Periodic planar-homeotropic anchoring realized by photoalignment for stabilization of chiral superstructures, *Adv. Opt. Mater.*, 2018, **6**, 1701163.
32 L. Zhang, L. Wang, U. S. Hiremath, H. K. Bisoyi, G. G. Nair, C. V. Yelamaggad, A. M. Urbas, T. J. Bunning and Q. Li, Dynamic orthogonal switching of a thermoresponsive self-organized helical superstructure, *Adv. Mater.*, 2017, **29**, 1700676.
33 R. Eelkema, M. M. Pollard, N. Katsonis, J. Vicario, D. J. Broer and B. L. Feringa, Rotational reorganization of doped cholesteric liquid crystalline films, *J. Am. Chem. Soc.*, 2006, **128**, 14397-14407.
34 T. Sasaki, R. Shimura, K. Kawai, K. Noda, M. Sakamoto, N. Kawatsuki and H. Ono, Alignment structures and diffraction properties of chiral nematic liquid crystal cells with periodically patterned photoalignment films, *Jpn. J. Appl. Phys.*, 2015, **55**, 12001.
35 A. Ryabchun, A. Bobrovsky, J. Stumpe and V. Shibaev, Electroinduced diffraction gratings in cholesteric polymer with phototunable helix pitch, *Adv. Optical Mater.*, 2015, **3**, 1462-1469.
36 R. L. Biagio, R. T. De Souza, L. R. Evangelista, R. R. de Almeida and R. S. Zola, Spontaneous striped pattern formation in thin chiral nematic liquid crystal layers, *J. Mol. Liq.*, 2018, **269**, 703-711.
37 J. Baudry, M. Brazovskaia, L. Lejcek, P. Oswald and S. Pirkl, Arch-texture in cholesteric liquid crystals, *Liq. Cryst.*,1996, **21**, 893-901.
38 A. Ryabchun and A. Bobrovsky, Cholesteric liquid crystal materials for tunable diffractive optics, *Adv. Opt. Mater.*, 2018, **6**, 1800335.
39 C. H. Lin, R. H. Chiang, S. H. Liu, C. T. Kuo and C. Y. Huang, Rotatable diffractive gratings based on hybrid-aligned cholesteric liquid crystals, *Opt. Express*, 2012, **20**, 26837-26844.
40 T. Nose, T. Miyanishi, Y. Aizawa, R. Ito and M. Honma, Rotational behavior of stripe domains appearing in hybrid aligned chiral nematic liquid crystal cells, *Jpn. J. Appl. Phys.*, 2010, **49**, 51701.
41 H. K. Bisoyi, T. J. Bunning and Q. Li, Stimuli-driven control of the helical axis of self-organized soft helical superstructures, *Adv. Mater.*, 2018, **30**, 1706512.
42 Y. Kim and N. Tamaoki, A photoresponsive planar chiral azobenzene dopant with high helical twisting power, *J. Mater. Chem. C*, 2014, **2**, 9258-9264.
43 A. Ryabchun, A. Bobrovsky, J. Stumpe and V. Shibaev, Rotatable diffraction gratings based on cholesteric liquid crystals with phototunable helix pitch, *Adv. Opt. Mater.*, 2015, **3**, 1273-1279.
44 L. L. Ma, W. Duan, M. J. Tang, L. J. Chen, X. Liang, Y. Q. Lu and W. Hu, Light-driven rotation and pitch tuning of self-organized cholesteric gratings formed in a semi-free film, *Polymers*, 2017, **9**, 295.
45 H. Wang, H. K. Bisoyi, X. Zhang, F. Hassan and Q. Li, Visible light-driven molecular switches and motors: recent developments and applications, *Chem. Eur. J.*, 2022, **28**, e202103906.
46 Y. Wang, A. Urbas and Q. Li, Reversible visible-light tuning of self-organized helical superstructures enabled by unprecedented light-driven axially chiral molecular switches, *J. Am. Chem. Soc.*, 2012, **134**, 3342-3345.
47 H. Wang, H. K. Bisoyi, B. X. Li, M. E. McConney, T. J. Bunning and Q. Li, Visible-light-driven halogen bond donor based molecular switches: from reversible unwinding to handedness inversion in self-organized soft helical superstructures, *Angew. Chem.*, 2020, **132**, 2706-2709.
48 H. Wang, H. K. Bisoyi, M. E. McConney, A. M. Urbas, T. J. Bunning and Q. Li, Visible-Light-Induced Self-Organized Helical Superstructure in Orientationally Ordered Fluids, *Adv. Mater.*, 2019, **31**, 1902958.
49 C. Rosini, S. Superchi, H. Peerlings and E. Meijer, Enantiopure dendrimers derived from the 1, 1'-binaphthyl moiety: a correlation between chiroptical properties and conformation of the 1, 1'-binaphthyl template, *Eur J. Org. Chem.*, 2000, **2000**, 61-71.
50 W. Zhang, A.A. Froyen, A.P. Schenning, G. Zhou, M.G. Debije, and L.T. de Haan, Temperature-Responsive Photonic Devices Based on Cholesteric Liquid Crystals, *Adv. Photonics Res.*, 2021, **2**, 2100016.
51 W. Helfrich, Deformation of cholesteric liquid crystals with low threshold voltage, *Appl. Phys. Lett.*, 1970, **17**, 531-532.
52 W. S. Choi, M. K. Kim, Effect of small liquid crystal molecules on the driving voltage of cholesteric liquid crystal displays, *Displays*, 2004, **25**, 195-199.